Absorption of NO_x Gases in Aqueous NaOH Solutions: Selectivity and Optimization

M. P. Pradhan and J. B. Joshi
Dept. of Chemical Technology, University of Mumbai, Matunga, Mumbai 400 109, India

A mathematical model is presented for multicomponent gas absorption with multiple reactions by considering the case of NO_x absorption in aqueous solution of NaOH. Procedures are developed for estimating the overall reaction rates and selectivity. The effects of temperature, pressure, and NO_x composition are examined. Optimum design strategy is suggested by proper configuration of the oxidation and absorption stages and by appropriate selection of levels of oxidation and absorption. A comparison between the model predictions and the performance of two operating plants is presented.

Introduction

Absorption of NO_x gases in aqueous solutions of sodium hydroxide and sodium carbonate is important in pollution abatement and in the manufacture of sodium nitrite. This case of absorption with chemical reaction is one of the most complex when compared with other absorption operations. First, the NO_x gas is a mixture of several components—NO, NO_2, N_2O_3, N_2O_4, and so on. These gases form HNO_2 and HNO_3 in the presence of water vapor. Second, several reversible and irreversible reactions occur in the gas phase. Third, the simultaneous absorption of many gases occurs and is accompanied by a chemical reaction.

For the process design of NO_x absorption towers, it is necessary to understand the combined effects of several equilibria, rates of mass transfer, and chemical reaction. Also, the liquid-phase reaction yields two products: sodium nitrite and sodium nitrate, of which sodium nitrite is commercially more important. Therefore, if the process design concurrently satisfies two objectives—conversion with respect to gas phase and the selectivity toward nitrite—the liability of the pollution problem can be advantageously converted into assets.

Mathematical models for the absorption of NO_x gases in alkaline solutions have been reported by Kameoka and Pigford (1977), Komiyama et al. (1982), Carta (1984), and Suchak et al. (1990). Some patent literature is also available on this subject. They have reported the factors (such as temperature, pressure, composition of NO_x gas, the partial pressures of oxygen and water in the gas phase) that influence the overall rate of absorption and the selectivity. Interestingly, all the factors that favor the rates of absorption hamper the selectivity, and vice versa. Therefore, it was thought desirable to understand the quantitative effects of all these factors and harness them for the optimum design in terms of equipment volume and selectivity. Such an exercise necessitates the steps of absorption and chemical reaction (oxidation of nitric oxide) to be carried out in different stages. Further, several configurations are possible in the arrangement of various stages of oxidation and absorption. The present article analyzes such configurations and presents a procedure for the optimum design.

The problem just presented involves multicomponent gas absorption with multiple reactions. A similar situation is encountered in the manufacture of nitric acid and has been systematically analyzed by Counce and Perona (1983) and Pradhan et al. (1997).

Mathematical Model

Determination of overall rate of absorption

Gas Phase Reactions. The NO_x gas is a mixture of various nitrogen oxides, namely, NO, NO_2, N_2O_3, N_2O_4, and so on (see Figure 1). Nitric oxide (NO) in the presence of oxygen undergoes irreversible oxidation to form NO_2. The rate of

---

Correspondence concerning this article should be addressed to J. B. Joshi.

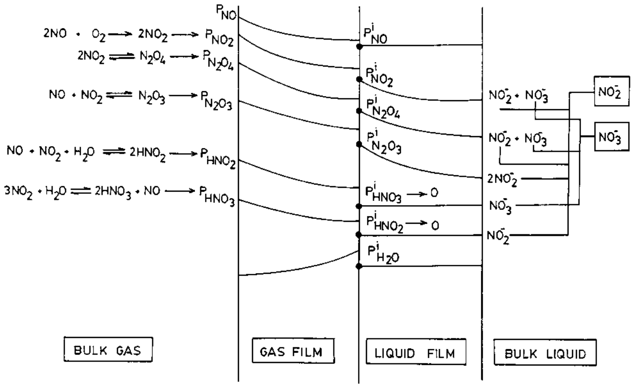

Figure 1. Mechanism of NO_x absorption in aqueous alkaline solutions.

oxidation is first order with respect to oxygen and second order with respect to NO.

The oxidation reaction is expressed as

$$2\,NO(g) + O_2(g) \xrightarrow{k_1} 2\,NO_2(g). \qquad (1)$$

Several reversible reactions prevail in the gas phase. Important reactions are given by the following equations:

$$2\,NO_2(g) \overset{K_2}{\rightleftharpoons} N_2O_4(g) \qquad (2)$$

$$NO(g) + NO_2(g) \overset{K_3}{\rightleftharpoons} N_2O_3(g) \qquad (3)$$

$$NO(g) + NO_2(g) + H_2O(g) \overset{K_4}{\rightleftharpoons} 2\,HNO_2(g) \qquad (4)$$

$$3\,NO_2(g) + H_2O(g) \overset{K_5}{\rightleftharpoons} 2\,HNO_3(g) + NO(g). \qquad (5)$$

The reaction rate constant is k_1 and the equilibrium constants $K_2 - K_5$ have been compiled by Joshi et al. (1985). These are given in Table 1.

The first and foremost exercise is to estimate the concentrations of all the gases at a given temperature and pressure. The concentrations are expressed in terms of moles of a component gas per mole of inerts. Thus we have eight components in the gas phase: NO, NO_2, N_2O_3, N_2O_4, O_2, H_2O, HNO_2, and HNO_3.

The equilibrium constants are given by the following equations:

$$K_2 = \frac{(Y_{N_2O_4})(Y_T)}{(Y_{NO_2})^2(P_T)} \qquad (6)$$

$$K_3 = \frac{(Y_{N_2O_3})(Y_T)}{(Y_{NO})(Y_{NO_2})(P_T)} \qquad (7)$$

$$K_4 = \frac{(Y_{HNO_2})^2(Y_T)}{(Y_{NO})(Y_{NO_2})(Y_{H_2O})(P_T)} \qquad (8)$$

$$K_5 = \frac{(Y_{HNO_3})^2(Y_{NO})(Y_T)}{(Y_{NO_2})^3(Y_{H_2O})(P_T)}. \qquad (9)$$

Table 1. Gas-Phase Reactions: Values of Rate and Equilibrium Constants

Equation No.	Equilibrium and Rate Constants, kN/m^2
1*	$\log_{10} k_1 = 652.1/T - 0.7356$
2**	$\log_{10} K_2 = 2993/T - 9.226$
3**	$\log_{10} K_3 = 2072/T - 7.234$
4**	$\log_{10} K_4 = 2051.17/T - 6.7238$
5**	$\log_{10} K_5 = 2003.8/T - 8.757$

*Bodenstein (1922).
**Schwartz and White (1981).

The total number of moles of the gas phase per mole of inerts is given by:

$$Y_T = Y_{NO} + Y_{NO_2} + Y_{N_2O_3} + Y_{N_2O_4} + Y_{HNO_3} + Y_{HNO_2} + Y_{H_2O} + Y_{O_2} + 1. \qquad (10)$$

Let us define three new parameters, namely Y^*_N, Y^*_{NO}, and $Y^*_{H_2O}$, where Y^*_N is the total moles of reactive nitrogen per mole of inerts, Y^*_{NO} is the total moles of divalent reactive nitrogen per mole of inerts, and $Y^*_{H_2O}$ is the total moles of water per mole of inerts. These quantities are given by the following equations:

$$Y^*_N = Y_{NO} + Y_{NO_2} + 2\,Y_{N_2O_4} + 2\,Y_{N_2O_3} + Y_{HNO_3} + Y_{HNO_2} \qquad (11)$$

$$Y^*_{NO} = Y_{NO} + Y_{N_2O_3} + 0.5\,Y_{HNO_2} - 0.5\,Y_{HNO_3} \qquad (12)$$

$$Y^*_{H_2O} = Y_{H_2O} + 0.5\,Y_{HNO_3} + 0.5\,Y_{HNO_2}. \qquad (13)$$

Substituting Eqs. 6–9 in Eqs. 10–13 and eliminating $Y_{N_2O_4}$, $Y_{N_2O_3}$, Y_{HNO_2}, and Y_{HNO_3}, we get

$$Y_T(Y^*_N - Y_{NO} - Y_{NO_2}) - Y_T^{1/2}\left[(K_4 P_T Y_{NO} Y_{NO_2} Y_{H_2O})^{1/2} + \left(K_5 P_T (Y_{NO_2})^3 \frac{Y_{H_2O}}{Y_{NO}}\right)^{1/2}\right] - 2\,P_T\left(K_2(Y_{NO_2})^2 - K_3 Y_{NO} Y_{NO_2}\right) = 0 \qquad (14)$$

$$Y_T(Y^*_{NO} - Y_{NO}) - 1/2\,Y_T^{1/2}\left[(K_4 P_T Y_{NO} Y_{NO_2} Y_{H_2O})^{1/2} - \left(K_5 P_T (Y_{NO_2})^3 Y_{H_2O}/Y_{NO}\right)^{1/2}\right] - K_3 P_T Y_{NO} Y_{NO_2} = 0 \qquad (15)$$

$$Y_T(Y^*_{H_2O} - Y_{H_2O}) - 1/2\,Y_T^{1/2}\left[(K_4 P_T Y_{NO} Y_{NO_2} Y_{H_2O})^{1/2} + \left(K_5 P_T (Y_{NO_2})^3 \frac{Y_{H_2O}}{Y_{NO}}\right)^{1/2}\right] = 0 \qquad (16)$$

$$Y_T^2 - Y_T(Y_{NO} + Y_{NO_2} + Y_{H_2O} + Y_{O_2} + 1) - Y_T^{1/2}\left[\left(K_5 P_T (Y_{NO_2})^3 \frac{Y_{H_2O}}{Y_{NO}}\right)^{1/2} + (K_4 P_T Y_{NO} Y_{NO_2} Y_{H_2O})^{1/2}\right] - \left[K_3 P_T Y_{NO_2} Y_{NO} + K_2 P_T (Y_{NO_2})^2\right] = 0. \qquad (17)$$

If Y_{O_2}, $Y^*_{H_2O}$, Y^*_{NO}, and Y^*_{N} are known, then the unknown variables are Y_T, Y_{NO}, Y_{NO_2}, and Y_{H_2O}. These four unknowns can be evaluated by solving the four nonlinear algebraic equations (Eqs. 14–17).

Rates of Gas-Phase Mass Transfer. The volumetric rates of gas-phase mass transfer are given by the following equations:

$$Rg_x = (k_G a)_x \left[p^o_x - p^i_x \right], \qquad (18)–(24)$$

where x is NO, NO_2, N_2O_3, N_2O_4, HNO_2, HNO_3, and H_2O. It can be noted that the reactions of nitrous and nitric acid vapors with NaOH can be considered to be instantaneous. Therefore, the interface partial pressures of HNO_2 and HNO_3 can be considered to be zero. The interface partial pressure of water was assumed to be equal to the vapor pressure over the given NaOH concentration and temperature.

It is obvious from Eqs. 18–24 that the interface partial pressures depend upon the values of the mass transfer coefficient $[(k_G a)_x]$ and hence the selectivity also depends upon $(k_G a)_x$.

Interface Equilibria. Since rates of the forward and backward reactions in Eqs. 2 and 3 are very high, the components NO, NO_2, N_2O_3, and N_2O_4 can be considered always to be in equilibrium. Therefore, the following equations hold at the interface:

$$K_2 = \frac{\left(p^i_{N_2O_4}\right)}{\left(p^i_{NO_2}\right)^2} \qquad (25)$$

$$K_3 = \frac{\left(p^i_{N_2O_3}\right)}{\left(p^i_{NO}\right)\left(p^i_{NO_2}\right)}. \qquad (26)$$

The reaction between an alkali and HNO_2 or HNO_3 has been assumed to be instantaneous. Therefore, there is no free HNO_3 and HNO_2 in the liquid phase, and the equilibrium vapor pressures of HNO_3 and HNO_2 ($p^i_{HNO_3}$ and $p^i_{HNO_2}$) are also zero. Vapor-pressure data of water over alkaline solutions have been reported in the literature (Perry and Chilton, 1984) as a function of temperature and concentration of an alkali.

$$p^i_{H_2O} = f(T, [\mathrm{NaOH}]). \qquad (27)$$

Liquid-Phase Reactions. Nitrogen oxides, when absorbed in an alkaline solution, form nitrite and nitrate ions. The following reactions occur in the liquid phase:

$$2NO_2(l) + 2OH^-(l) \longrightarrow NO_2^-(l) + NO_3^-(l) + H_2O(l) \qquad (28)$$

$$N_2O_3(l) + 2OH^-(l) \longrightarrow 2NO_2^-(l) + H_2O(l) \qquad (29)$$

$$N_2O_4(l) + 2OH^-(l) \longrightarrow NO_2^-(l) + NO_3^-(l) + H_2O(l) \qquad (30)$$

$$HNO_2(l) + OH^-(l) \longrightarrow NO_2^-(l) + H_2O(l) \qquad (31)$$

$$HNO_3(l) + OH^-(l) \longrightarrow NO_3^-(l) + H_2O(l). \qquad (32)$$

It can be seen from Eqs. 28–32 that the nitric oxide (NO) does not react with NaOH on its own. For a reaction to occur, one mole of NO needs one mole of NO_2 to form either N_2O_3 or HNO_2 (according to Eqs. 3 and 4), and the subsequent reactions are given by Eqs. 29 and 31, respectively. The decrease in NO concentration can also occur via gas-phase oxidation (Eq. 1) to form NO_2. The product NO_2 reacts with NaOH, as already mentioned, according to Eq. 28. In addition to these reactions, NO_2 gets converted into N_2O_4 and HNO_3 (Eqs. 2 and 5). The products N_2O_4, HNO_3, and NO_2 itself react with NaOH according to Eqs. 30, 32, and 28, respectively. Because of these three reactions, the overall rate of NO_2 absorption is much higher than NO absorption. However, the reactions that enhance the rate of NO_2 absorption unfortunately result in poorer selectivity. It can be seen from Eqs. 28, 30, and 32 that the formation of nitrite and nitrate is equimolar.

Mass Transfer with Chemical Reaction in the Liquid Film. The absorption of NO_2, N_2O_3, and N_2O_4 is accompanied by a chemical reaction within the liquid film. The volumetric rates of absorption in the liquid film are (Joshi et al., 1985):

$$Ra_{NO_2} = aH^{3/2}_{NO_2}\left[2/3\,(kD)^{1/2}_{NO_2}\right]\left(p^i_{NO_2}\right)^{3/2} \qquad (33)$$

$$Ra_{N_2O_4} = aH_{N_2O_4}\left[(kD)^{1/2}_{N_2O_4}\right] p^i_{N_2O_4} \qquad (34)$$

$$Ra_{N_2O_3} = aH_{N_2O_3}\left[(kD)^{1/2}_{N_2O_3}\right] p^i_{N_2O_3}. \qquad (35)$$

Mass Balance Across the Interface. It can be seen that the transfer of various components occurs across the interface. The mass balance across the interface gives:

Tetravalent nitrogen oxides

$$\left(Rg_{NO_2} - Ra_{NO_2}\right) = 2\left(Ra_{N_2O_4} - Rg_{N_2O_4}\right) + \left(Ra_{N_2O_3} - Rg_{N_2O_3}\right). \qquad (36)$$

Divalent nitrogen oxides

$$Rg_{NO} = \left(Ra_{N_2O_3} - Rg_{N_2O_3}\right). \qquad (37)$$

It is interesting to note that, for any one component, the gas-phase and liquid-phase rates of mass transfer do not need to be equal. This happens because of the equilibria. Therefore, because of the liquid-phase transfer of HNO_2 and N_2O_3, and because of the equilibria at the interface (with concentration zero), the concentration of NO at the interface is different from the bulk concentration. As a result, transfer of NO occurs in the gas phase even though there is no chemical reaction between NO and NaOH.

Estimating the overall reaction rate

Equations 6 to 37 form the basis for the estimation of the overall rate of reaction. It should be noted that there are 23 unknowns. These are:

1. Eight partial pressures in the gas phase: p^o_{NO}, $p^o_{NO_2}$, $p^o_{N_2O_4}$, $p^o_{N_2O_3}$, $p^o_{O_2}$, $p^o_{H_2O}$, $p^o_{HNO_2}$, and $p^o_{HNO_3}$.
2. Seven rates of gas-phase mass transfer: Rg_{NO}, Rg_{NO_2}, $Rg_{N_2O_3}$, $Rg_{N_2O_4}$, Rg_{HNO_3}, Rg_{HNO_2}, Rg_{H_2O}.

3. Five partial pressures of gas phase at the interface: p^i_{NO}, $p^i_{NO_2}$, $p^i_{N_2O_4}$, $p^i_{N_2O_3}$, $p^i_{H_2O}$.

4. Three rates of mass transfer with chemical reaction in the liquid film: Ra_{NO_2}, $Ra_{N_2O_4}$, $Ra_{N_2O_3}$.

However, the number of equations are nineteen (Eqs. 6–9, 18–27, 33–37). Therefore, the values of four variables are needed to solve the problem. We thus specify the values of Y^*_{NO}, Y^*_N, $Y^*_{H_2O}$, and Y_{O_2} (the methodology for this specification is described in the next subsection). With these four specified variables, the values of the other nineteen variables can be estimated by solving the nineteen equations. The solution of Eq. 27 is directly available. The other eighteen equations were reduced to the following two nonlinear algebraic equations, which were solved by the matrix inversion method:

$$A_1\left(p^i_{NO_2}\right)^3 + A_2\left(p^i_{NO_2}\right)^2\left(p^i_{NO}\right) + A_3\left(p^i_{NO_2}\right)^{3/2}\left(p^i_{NO}\right) + A_4\left(p^i_{NO_2}\right)\left(p^i_{NO}\right)^2 + A_5\left(p^i_{NO}\right)\left(p^i_{NO_2}\right) + A_6\left(p^i_{NO}\right) = 0$$

$$B_1\left(p^i_{NO}\right)^2 + B_2\left(p^i_{NO}\right)^2\left(p^i_{NO_2}\right) + B_3\left(p^i_{NO}\right) + B_4\left(p^i_{NO_2}\right)^3 = 0,$$

where the constants $A_1 - A_6$ and $B_1 - B_6$ have been given by Suchak et al. (1990).

Model for column performance

In the preceding subsection, we gave for estimating the concentrations of all the components and the rates of gas and liquid phase reactions. For this purpose, the values of Y^*_{NO}, Y^*_N, $Y^*_{H_2O}$, and Y_{O_2} are needed. Therefore, the model for column performance was developed in terms of these variables. For the case of countercurrent absorption in a packed column, the following assumptions were made:

1. Gas and liquid phases move in a plug-flow manner.
2. Liquid holdup is uniform throughout the column. Therefore, the values of effective interfacial area and mass-transfer coefficient are also uniform throughout the column.
3. Gases follow ideal-gas behavior.
4. There are no concentration and temperature gradients in the radial direction.
5. The column is operated under steady-state conditions.
6. The liquid flow rates were kept sufficiently high in such a way that the per-pass temperature rise was less than 2°C. Therefore, as a first approximation isothermal conditions were assumed. We thought it desirable that the problems of conversion and selectivity should be understood first in view of the complexity of the multicomponent absorption with multiple reactions. The analysis can then be extended to non-isothermal conditions.

Mass Balance for the Gas Phase. Mass balance across a differential height *dh* gives (Figure 2):

1. Balance of reactive divalent nitrogen:

$$\frac{dY^*_{NO}}{dh} = -\frac{S}{G}\left(k_1\left(P^o_{NO}\right)^2 P^o_{O_2}\epsilon_G + Rg_{NO} + Rg_{N_2O_3} + 0.5\left(Rg_{HNO_2} - Rg_{HNO_3}\right)\right). \quad (38)$$

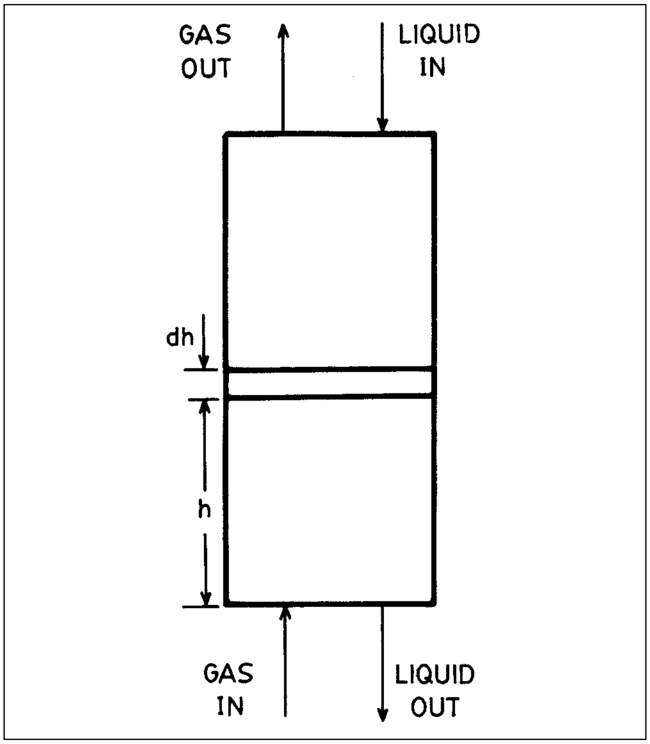

Figure 2. Packed column.

2. Balance of total reactive nitrogen:

$$\frac{dY^*_N}{dh} = -\frac{S}{G}\left(Rg_{NO} + Rg_{NO_2} + 2\,Rg_{N_2O_3} + 2\,Rg_{N_2O_4} + Rg_{HNO_3} + Rg_{HNO_2}\right). \quad (39)$$

3. Balance of water (both reactive and free):

$$\frac{dY^*_{H_2O}}{dh} = -\frac{S}{G}\left(Rg_{H_2O} + 1/2\,Rg_{HNO_3} + 1/2\,Rg_{HNO_2}\right). \quad (40)$$

4. Oxygen balance:

$$\frac{dY_{O_2}}{dh} = -\frac{1}{2}\frac{S}{G}\left(k_1\left(P^o_{NO^2}\right)\left(P^o_{O_2}\right)\epsilon_G\right). \quad (41)$$

Mass Balance for the Liquid Phase

5. Hydroxide ion balance:

$$\frac{dX_{OH^-}}{dh} = \frac{S}{L}\left[2\left(Ra_{N_2O_4} + Ra_{N_2O_3}\right) + Rg_{HNO_3} + Rg_{HNO_2} + Ra_{NO_2}\right]. \quad (42)$$

6. Balance of nitrate ion:

$$\frac{dX_{NO_3^-}}{dh} = -\frac{S}{L}\left(Ra_{N_2O_4} + Rg_{HNO_3} + 1/2\,Ra_{NO_2}\right). \quad (43)$$

7. Balance of nitrite ion:

$$\frac{dX_{NO_2^-}}{dh} = -\frac{S}{G}\left(Ra_{N_2O_4} + 2\,Ra_{N_2O_3} + Rg_{HNO_2} + 1/2\,Ra_{NO_2} \right). \tag{44}$$

Equations 38–44 are coupled first-order differential equations. For the solution of these equations, seven inlet conditions (at $h = 0$) are needed. The starting point for the column design is the specification of the quantity and quality of the gas stream. For this purpose (see Figure 2), the molar flow rate of the inert, the composition of oxygen, and total reactive nitrogen (G, Y_{O_2}, and Y_N^*, respectively) and the composition of water (Y_{H_2O}) are considered to be specified. The total reactive nitrogen consists of divalent and tetravalent forms, and we need to know Y_{NO}^* in Y_N^*. The analysis procedure was given by Suchak et al. (1990). In regard to water composition, as a first approximation, the concentrations of HNO_3 and HNO_2 were considered to be negligible or $Y_{H_2O}^*$ was assumed to be the same as Y_{H_2O}. Thus, at the column inlet four boundary conditions for Y_{O_2}, Y_{NO}^*, Y_N^*, and $Y_{H_2O}^*$ are known. From this knowledge, the procedure was described, in the preceding subsection, for estimating the bulk and interface partial pressures of various components and the rates of gas and liquid phase mass transfer. These rates were substituted in Eqs. 38 to 44.

In regard to the boundary conditions for the liquid phase, these were adjusted by trial and error. The problem definition specifies the outlet gas composition from the column. It also specifies the inlet composition of the liquid stream (which may be an aqueous solution of NaOH or known amounts of nitrite and nitrate). Thus the boundary conditions are known at the outlet. Therefore, for starting the integration of Eqs. 42 to 44, the values of X_{OH^-}, $X_{NO_3^-}$, and $X_{NO_2^-}$ were adjusted to satisfy the outlet boundary conditions.

Estimation of design parameters

While estimating the overall rate of reaction (the subsection on estimating the overall reaction rate), the values of the design parameters, such as effective interfacial area and mass-transfer coefficient, are needed. These were estimated by using the following correlations. Details pertaining to these correlations were given by Suchak et al. (1990).

1. Effective interfacial area:

$$a = \frac{m_1 V_L^{m_2}\left(\dfrac{dp}{1{,}000}\right)^{m_3}}{\epsilon^3} \tag{45}$$

where m_1, m_2, and m_3 are constants, and ϵ is the voidage. The constants and the voidage depend on the type and material of construction of the packing used. Stainless-steel pall rings were considered to be packings in the study. The values for m_1, m_2, m_3, and ϵ for a variety of packings were given by Jethani et al. (1992).

Table 2. Values of $H\sqrt{(kD)}$ for Various NO_x Components at 25°C and Activation Energy

Component	$H\sqrt{(kD)}$ kmol/(m^2·KN/m^2·s)	Activation Energy (E/R) kcal/kmol
NO_2	2×10^{-7}	-4564.16
N_2O_3	2.5×10^{-4}	-4564.16
N_2O_4	8.1×10^{-6}	1285.3

2. Gas-side mass-transfer coefficient:

$$\frac{(k_G RT)\,L_T}{D_G} = 0.553\left[\frac{(P_M L_T)^{(1/3)} L_T \rho_G}{\mu_G}\right]^{0.62} (Sc_G)^{1/3}\left(\frac{P_T}{P_I}\right)$$

$$P_M = \left(\frac{f a_p}{6(\epsilon - \epsilon_L)^4}\right) V_G^3, \tag{46}$$

where L_T depends on the type of packing; $L_T = 0.5\,dp$ for ceramic raschig rings, $L_T = 0.25\,dp$ for Intalox saddles, and $L_T = 0.1\,dp$ for stainless-steel pall rings.

3. Mass-transfer with chemical reaction.

The rates of mass transfer with chemical reaction in the liquid phase for NO_2, N_2O_4, and N_2O_3 are given by Eqs. 33, 34 and 35, respectively. For the estimation of these rates, the values of physicochemical parameter $H_x\sqrt{(kD)_x}$ were estimated by several workers. These results were analyzed by Joshi et al. (1985) and Suchak et al. (1990). These authors have recommended a set of values, as shown in Table 2.

Results and Discussion

Parametric sensitivity

In the subsection titled "Model for column performance," procedures were described for estimating the concentrations and reaction rates of various components, such as NO, NO_2, N_2O_3, N_2O_4, HNO_2, HNO_3. It was also pointed out that, for achieving higher levels of selectivity, it is desired that the NO_2 gets reacted according to Eqs. 29 and 31 (where only nitrite is formed) and not according to Eqs. 28, 30, and 32. In order to achieve this, the concentrations of N_2O_4 and HNO_3 need to be as low as possible. These estimations can be carried out on the basis of equilibrium constants $K_2 - K_5$ (Table 1). Joshi et al. (1985) have shown that the relative proportion of N_2O_4 and HNO_3 in NO_2^* (total tetravalent nitrogen oxides) is less (or NO_2 is more) at low concentrations of NO_2^* and at high temperatures.

The foregoing discussion emphasizes the following important points for getting better selectivity: (1) the selectivity increases with a decrease in mole fraction of total reactive nitrogen (Eq. 11); and (2) in the total reactive nitrogen (N^*), the relative proportion of NO_2^* should be low compared with NO^*. The selectivity increases with an increase in the ratio of NO^*/NO_2^*.

Thus, it is clear that the rate and selectivity have contrasting demands on the NO^*/NO_2^* ratio and Y_N^*. In addition, the temperature and total pressure are two more important parameters. For a given pressure, the mole fraction of water

$(Y^*_{H_2O})$ increases with an increase in temperature. Therefore, Y^*_N decreases. As a result, $Y_{N_2O_4}$ also decreases for a given $Y^*_{NO_2}$. However, an increase in $(Y^*_{H_2O})$ may favor the formation of HNO_3 at high temperature and reduce the selectivity.

As with temperature, the effect of pressure is multifold. For a given temperature, an increase in pressure decreases $(Y^*_{H_2O})$; however, it increases Y^*_N and $Y_{N_2O_4}$. In view of interdependent relationships, let us establish the quantitative relationships before creating the design and overall optimization. For this purpose, simulation studies were carried out for a packed column, shown in Figure 2. The details of the design parameters (column diameter, packing size, type and material of construction, effective interfacial area, and gas-side mass-transfer coefficient) and operating parameters (flow rate and composition of gas, superficial liquid velocity) follow:

1. Column diameter = 1.9 m.
2. Type of packing = stainless-steel pall rings.
3. Diameter of packing = 12.7 mm.
4. Superficial liquid velocity = 4 mm/s.
5. Total NO_x at the inlet of packed column = 91,000 ppm.
6. Flow rate of inert = 0.05175 kmol/s.
7. Oxygen to total NO_x ratio at the inlet of the column = 0.82.
8. Total moles of gas/kmol of inert = 1.41.
9. Average molecular weight of gas = 27.80.
10. Total reactive nitrogen/kmol of inert = 0.1285.
11. Effective interfacial area = 375 m^2/m^3.
12. True gas-side mass-transfer coefficient $k_G a = 0.0116$ kmol/(m^3s(KN/m^2)).

Lean NO_x gas was introduced at the bottom and aqueous NaOH solution from the top. The liquid flow rate was sufficient to wet the packings. Therefore, the corresponding liquid flow rate was high and the per-pass conversion of NaOH was low. The inlet and outlet concentrations were about 25% and 24% (w/w), respectively; such low levels of per-pass conversion also ensured practically isothermal conditions. The simulation studies were carried out over a wide range of NO^*/NO_2^* ratio (90 to 0.5), temperature (30 to 65°C), Y^*_N (91×10^{-3} to 3×10^{-3}) and pressure (0.1 to 0.6 MPa).

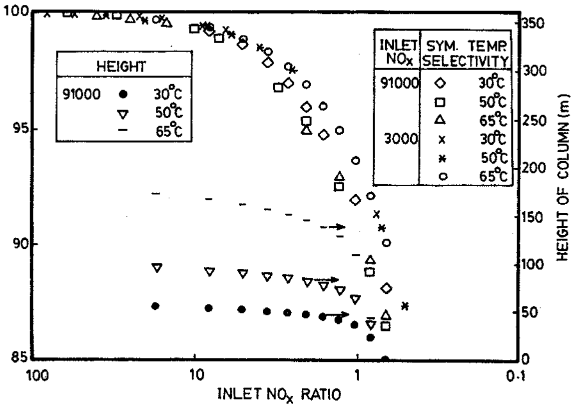

Figure 4. Effect of temperature.

Total inlet NO_x and NO^*/NO_2^* ratio on selectivity and packed height; inlet concentration of total NO_x = 91,000 ppm; outlet concentration of NO_x = 2500 ppm; pressure = 0.1 MPa; $b = 0.82$.

Figure 3 shows the effect of NO^*/NO_2^* ratio on the packed height for different levels of outlet NO_x. It can be seen that the packed height and outlet NO_x decrease with a decrease in the NO^*/NO_2^* ratio. This is because of the enhanced rates of reaction. However, the selectivity decreases from 99.97% to 86% when the ratio is decreased from 90 to 0.5. Figure 4 shows the effect of temperature and Figure 5 shows the effect of total pressure. From Figure 4 it can be seen that the packed height decreases with a decrease in temperature. Similarly, in Figure 5 it can be seen that the packed height decreases with an increase in pressure.

Regarding selectivity, it decreases with a decrease in pressure, as shown in Figure 5 and Table 3A. It was pointed out earlier that $(Y^*_{H_2O})$ increases and $Y_{N_2O_4}$ decreases with a decrease in pressure. Out of these two mole fractions, the effect of $(Y^*_{H_2O})$ was found to be dominant. It favors the formation of HNO_3, and hence poorer selectivity. It can be pointed out that, though there is a definite trend in the relationship of selectivity and pressure, the extent of variation in selectivity is nominal when the NO^*/NO_2^* ratio is high.

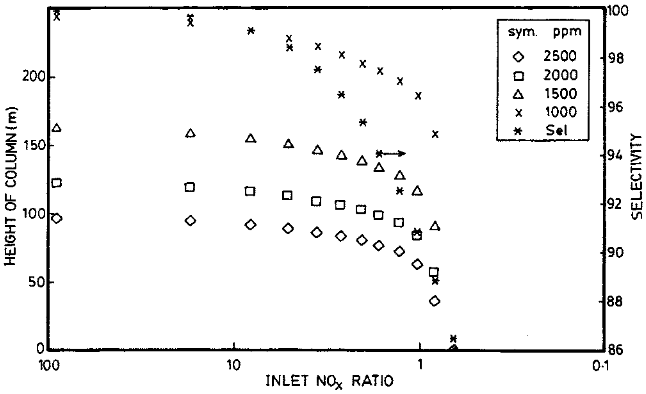

Figure 3. Effect of NO^*/NO_2^* ratio on selectivity and packed height for different levels of ppm.

Inlet concentration of total NO_x = 91,000 ppm; temperature = 50°C; pressure = 0.1 MPa; $b = 0.82$.

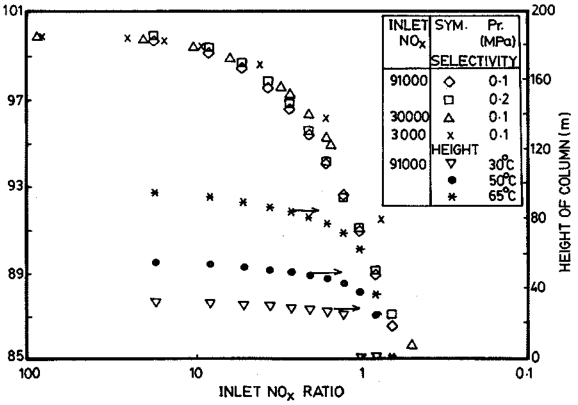

Figure 5. Effect of pressure.

Total inlet NO_x and NO^*/NO_2^* ratio on selectivity and packed height; outlet concentration of NO_x = 2500 ppm; temperature = 50°C; $b = 0.82$.

Table 3A. Effect of NO^*/NO_2^* Ratio, Total NO_x Concentration and Pressure on the Selectivity of Nitrite

		Pressure = 0.1 MPa			Temperature = 50°C				
		Temperature			Pressure				
Total NO_x (ppm)	Inlet Ratio	30°C	50°C	65°C	0.011 MPa	0.033 MPa	0.1 MPa	0.2 MPa	0.4 MPa
91000	17.2	99.73	99.66	99.65	—	99.59	99.66	99.72	99.89
	3.55	97.84	97.49	97.65	—	97.90	97.49	97.51	97.79
	1.023	91.96	90.81	91.35	—	90.00	90.81	90.92	91.05
30000	17.2	99.75	99.71	99.69	—	99.60	99.71	99.79	—
	3.55	98.04	98.22	97.98	—	98.0	98.22	98.13	—
	1.023	92.51	92.89	92.73	—	92.05	92.89	93.87	—
10000	17.2	99.77	99.72	99.70	99.65	99.67	99.72	99.85	—
	3.55	98.28	98.22	98.20	98.0	98.08	98.22	98.35	—
	1.023	93.26	93.27	93.43	92.65	93.05	93.27	93.65	—
3000	17.2	99.98	99.72	99.70	99.55	99.61	99.72	—	—
	3.55	98.43	98.32	98.27	98.04	98.22	98.32	—	—
	1.023	93.72	93.67	93.67	93.12	93.47	93.67	—	—

Regarding temperature, clear trends were not observed (Table 3A and Figure 4). One important point emerges from the foregoing discussion: out of the four parameters, that is, the ratio NO^*/NO_2^*, Y_N^*, pressure, and temperature, the ratio is the dominant parameter (Figures 4, 5, and Table 3A). Therefore, it will be interesting to note the values of NO^*/NO_2^* ratio for a given selectivity. For 99% selectivity, the results are given in Table 3B. As expected, the ratio increases with an increase in concentration of the NO_x (Y_N^*) and a decrease in pressure. For a given pressure and temperature, the variation in Y_N^* does not affect ($Y_{H_2O}^*$). However, $Y_{N_2O_4}$ increases with Y_N^* and reduces the selectivity. The effects of pressure and temperature were described earlier.

Since the NO^*/NO_2^* ratio was found to be the dominant parameter, we thought it desirable to investigate its sensitivity on the selectivity. The results are given in Figure 6. We can see that the demand on the ratio substantially decreases with a decrease in selectivity. The effect of the mole fraction of the total NO_x is also shown in Figures 4 and 5. As can be seen, at a given ratio of NO^*/NO_2^*, the selectivity increases with a decrease in the mole fraction of NO_x. It can be pointed out that the effects of the mole fraction and total pressure cannot be combined in a simple way in terms of the partial pressure of NO_x. This is because of the interlinked complex equilibria given by Eqs. 6 to 9.

Before closing this section, let us investigate the sensitivity of one more parameter: NaOH concentration. In Figures 3 to 6, the liquid flow rate was selected so as to wet the packings. For this flow rate, over the range of variables covered, the per-pass conversion of NaOH was always less than 4%. We used a recycle loop to investigate the effect of NaOH concentration, as shown in Figure 7a. The reaction and absorption heats were removed in the exchanger in the recycle loop. The concentration of NaOH could be adjusted by varying the recycle ratio, and the material balance was established by the following procedure.

Table 3B. Effect of NO_x Concentration, Temperature, and Pressure on the Critical Ratio

Total NO_x (ppm)	Total Pressure = 0.1 MPa			Temperature = 50°C	
	$T = 30°C$	$T = 50°C$	$T = 65°C$	$P = 0.2$ MPa	$P = 0.4$ MPa
91,000	6.91	7.67	7.67	6.58	6.28
30,000	6.14	6.5	6.5	6.14	5.52
10,000	5.67	6.14	6.14	5.45	4.88
3000	5.65	5.67	5.82	5.32	4.72
1000	5.62	5.62	6.14	5.17	4.56

Note: Other details are given the numbered list in the third section.

From the figure it can be seen that the stream A gets divided into two streams B and C, of which the net output stream is B and the recycle stream is C:

$$L_C = L_A - L_B, \tag{47}$$

where L is the molar flow rate of water which is an inert. The concentration of NaOH in all three streams is the same, and it can be varied by changing the recycle ratio. At the top, the recycle stream C meets the fresh stream E to give the total feed D:

$$L_D = L_E + L_C. \tag{48}$$

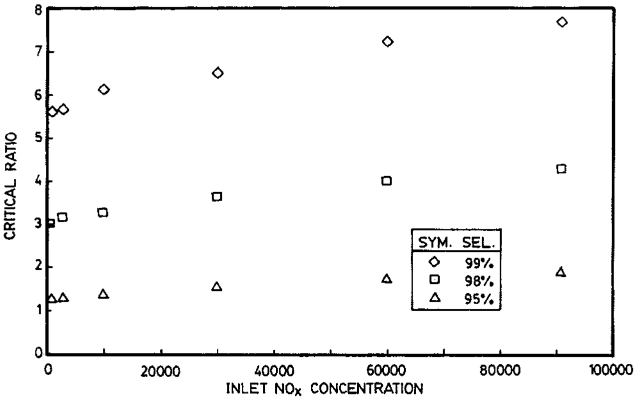

Figure 6. Effect of total NO_x on critical ratio for given selectivity.

Temperature 50°C; pressure = 0.1 MPa; $b = 0.82$.

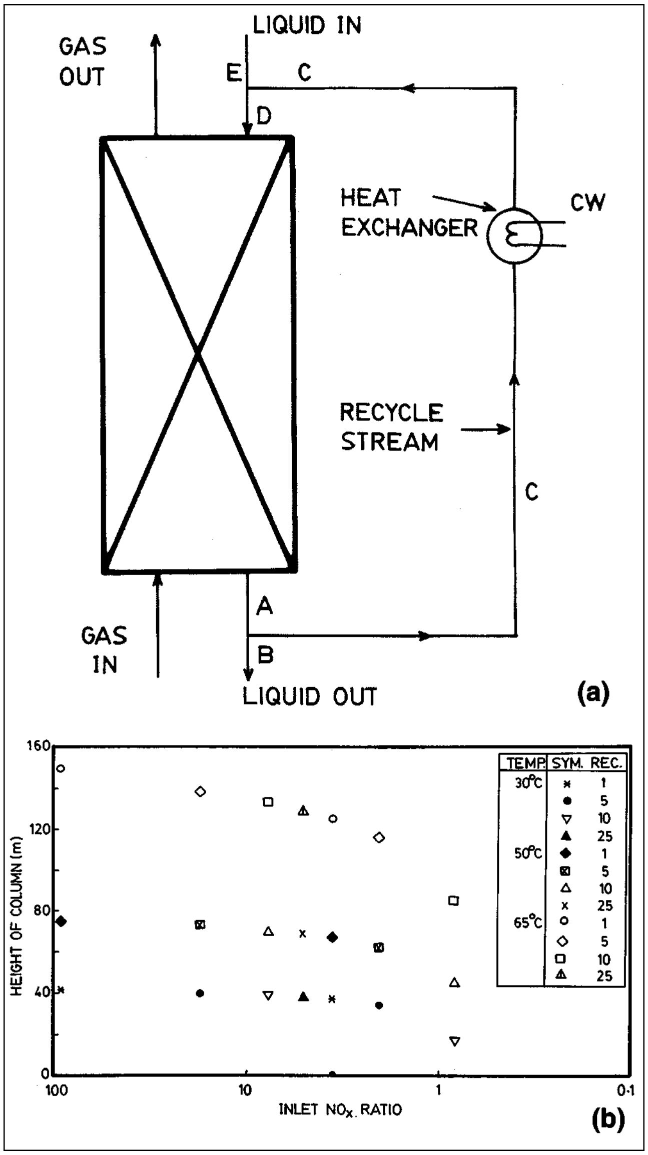

Figure 7. (a) Packed column with recycle loop; (b) effect of NO*/NO$_2^*$ ratio on packed height under recycle condition for different temperature.

Inlet concentration of total NO$_x$ = 91,000 ppm; outlet concentration of NO$_x$ = 2500 ppm; pressure = 0.1 MPa; b = 0.82.

The mass balance with respect to various components is given by:

$$(LX_{\mathrm{OH}^-})_D = (LX_{\mathrm{OH}^-})_E + (LX_{\mathrm{OH}^-})_C \tag{49}$$

$$(LX_{\mathrm{NO}_2^-})_D = (LX_{\mathrm{NO}_2^-})_E + (LX_{\mathrm{NO}_2^-})_C. \tag{50}$$

The calculation procedure was carried out according to the following steps: (1) the liquid flow rate in the column was selected according to the hydrodynamic calculations of the packed column (say, the superficial velocity of liquid phase is 4 mm/s). This gives the values of L_D and L_A; (2) the concentration of NaOH in the fresh feed was taken as 25% (w/w); (3) the concentration of NaOH in the net product B was assumed; (4) the overall mass balance across the column gives

$$G[(Y_{\mathrm{N}}^*)_{\mathrm{in}} - (Y_N^*)_{\mathrm{out}}] = L_E(X_{\mathrm{OH}^-})_E - L_B(X_{\mathrm{OH}^-})_B, \tag{51}$$

where L_E and L_B are either the same or any difference can be estimated from the amount of water in the inlet and outlet gas streams. This balance gives the value of L_B; (5) the value of L_A from step 1, and L_B from step 4 fixes the recycle ratio according to Eq. 47; (6) steps 3 to 5 were repeated to get a wide range of the NaOH concentration.

The effect of the NaOH concentration on the packed height is shown in Figure 7b. It can be seen that the required height is practically independent of the NaOH concentration. This is because the NaOH concentration does not appear in the rate calculations (see the subsection on estimating the overall reaction rate). The only expected effect was from the possible evaporation/condensation of water in the column. It can be emphasized that these results cannot be extrapolated to zero NaOH concentration. The reactions of HNO_2 and HNO_3 with NaOH are instantaneous. In the absence of NaOH, however, HNO_2 decomposes to HNO_3, and the subsequent reaction with NaOH yields only nitrate. In fact, this method can be used for the selective manufacture of $NaNO_3$. In this case, the scrubbing liquid is kept at pH ≤ 7 by carefully dosing NaOH in the recycle loop.

Comparison with plant data

Before undertaking the exercise of optimization, we thought it desirable to confirm the validity of the mathematical model developed in the section on the mathematical model and the results presented in the preceding subsection. For this purpose, the absorption systems of the two operating plants were simulated. In one case, the column had a 500-mm ID and 4-m packed height (total height 5000 mm). Stainless-steel 304 (16-mm) pall rings were used as packing. The column was operated in a continuous countercurrent mode. The column was used for pollution abatement for a gas stream from a nitric acid plant. The volumetric flow rate of the stream was measured using a precalibrated orifice meter.

Aqueous sodium hydroxide (initial concentration 20% w/w) was prepared in a 1000-L stainless-steel 304 vessel. The solution was passed through a precalibrated rotameter and the superficial liquid velocity was 3 mm/s. The temperature of the solution was maintained within ± 1°C. The discharge liquid from the column was returned to the same 1000-L vessel. The concentration of NaOH decreased with respect to time. When NaOH was reduced to $\leq 0.2\%$ (w/w), the liquor ($NaOH + NaNO_2 + NaNO_3$) was discharged and fresh solution added. This is shown in Figure 8.

The total gas flow rate was $2.16 \cdot 10^{-3}$ kmol/s (NO* = 6560 ppm, NO_2^* = 330 ppm, $O_2 = 1.03 \cdot 10^{-4}$ kmol/s). The method of analysis was given by Suchak et al. (1991). The total pressure was essentially atmospheric. The temperature variation was within 1°C along the length of the column. The selectivity was found to be 98.6%, which was found to be in close agreement with the predicted value of 98.94%.

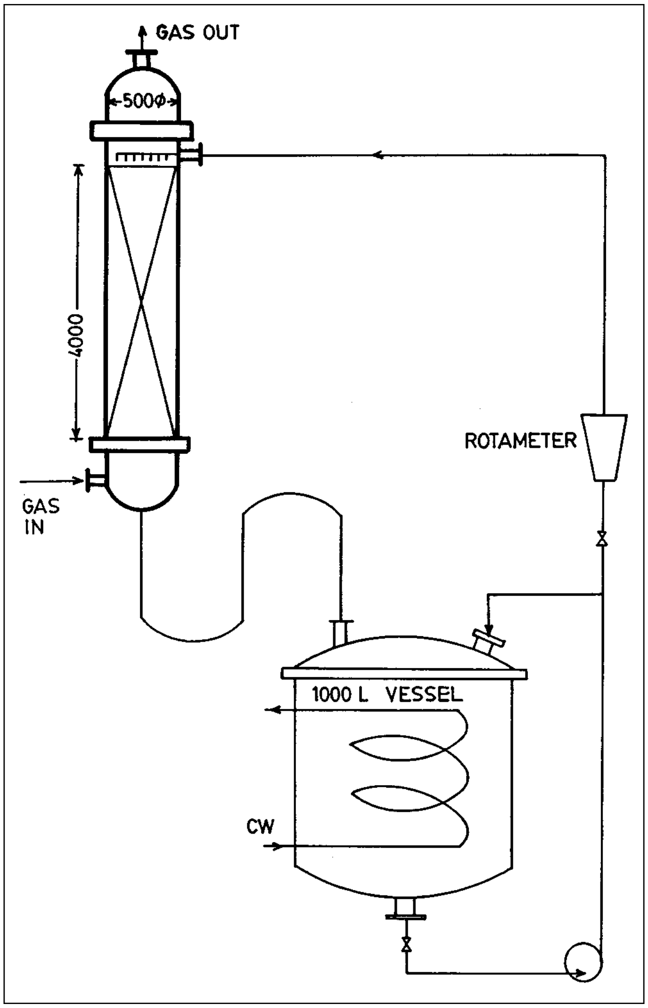

Figure 8. The plant setup.

In a second operating plant, the absorption system was used for the manufacture of $NaNO_2$. In the first case, the principal objective was pollution abatement, and small quantities of $NaNO_2$ were generated. In the second case, the absorption was also carried out in a stainless-steel 304 packed column of 150-mm ID and 3000-mm packed height. Stainless-steel 304 (16-mm) pall rings were used as packings. Further details were given by Suchak et al. (1990). The total flow rate of inert was $5.37 \cdot 10^{-5}$ kmol/s, the flow rate of NO_x gas was $2.51 \cdot 10^{-5}$ kmol/s, and the flow rate of gas was $9 \cdot 10^{-5}$ kmol/s. The divalent to tetravalent nitrogen oxides was 2.5. The NaOH circulation system was similar to that in Figure 8, except the heat exchanger was placed at the pump outlet for the removal of heat. The superficial liquid velocity was 6 mm/s. In this case, NO_x was 174,000 ppm in the presence of air and 467,000 ppm in the absence of air. The column was operated at essentially atmospheric pressure and at 50°C. The temperature variation along the column height was within 2°C. The selectivity was found to be 91.07% in the absence of air and 93.0% in the presence of air. The predicted values were found to be 90.2% and 93.6%, respectively. It can be seen that there is excellent agreement between the model predictions and the plant performance.

Rate of oxidation vs. the rate of absorption

It is crucial to understand the relative importance of gas phase oxidation reaction and the rate of mass transfer. While estimating these packed heights in Figures 3, 4, and 5, one very important observation was made. For a given NO^*/NO_2^* ratio, the tetravalent nitrogen oxides are absorbed at a very short distance from the entrance. At the beginning of packed section, the rate of absorption is high as compared to the rate of oxidation. The rate decreases sharply with an increase in height, though additional quantities of NO_2^* are formed. Finally the rates of oxidation and absorption become equal and the corresponding levels of NO_2^* (in the gas phase) are very low. Table 4 lists both the total height and the absorption height (absorption height was defined as the height at which the rate of absorption is at least five times the rate of oxidation). At this condition, the extent of NO_2^* absorption was found to be more than 95%. We can see in Table 4 that most of the column volume is used for oxidation, with a relatively small volume used for absorption. This situation is obviously uneconomical, because the packed volume is used for oxidation. The alternative economical choice is to use an empty

Table 4. Comparison Between Height of Absorption and Total Height of Column

Inlet NO^*/NO_2^* Ratio	Temperature 30°C		Temperature 50°C		Temperature 65°C	
	Height of		Height of		Height of	
	Absorption	Packed	Absorption	Packed	Absorption	Packed
90	33.6	108	19.75	225	13.18	428
17.2	33	105	19	221	12.7	418
8.1	32	102	19	215	11.72	407
5.07	34	96	17.5	210.5	10.58	397
3.55	34	94	16.7	205	9.13	388
2.64	33	91	15.45	201	7.18	379
2.03	32	89	14	196	4.43	372
1.6	30	88	12	193	0.55	365
1.28	26	86	7.57	189	0.05	352
1.022	23	85	0.62	185	0.05	329
0.82	9.83	84	0.73	157	0.05	262
0.65	0.65	0.14	0.05	0.74	0.05	0.74

Note: Total concentration of inlet $NO_x = 91{,}000$ ppm; total concentration of outlet $NO_x = 1000$ ppm; pressure = 0.1 MPa; $b = 0.82$.

section for oxidation so that expensive packings are eliminated and the volume occupied by the packings is also used for oxidation. However, we must be careful that the extent of oxidation is less than or equal to the critical level of NO^*/NO_2^* (at the corresponding values of temperature, Y_N^*, and pressure).

It will be interesting to compare the column volumes needed for the two cases: (1) oxidation and absorption carried out in two separate sections, and (2) oxidation and absorption carried out simultaneously.

Case 1: Oxidation Section. The following assumptions have been made: (1) plug-flow behavior for the gas phase; (2) isothermal conditions; (3) ideal gas behavior; and (4) the variation in the volumetric flow rate has also been assumed to be negligible. This assumption is reasonable because the total NO_x is less than 10%.

The oxidation reaction is given by Eq. 1. The rate of oxidation is first order in O_2 and second order in NO:

$$-\frac{dp_{NO}}{dt} = k_p p_{NO}^2 p_{O_2} \tag{51}$$

$$= k_p (p_{NO})_O^3 (1-\alpha)^2 \left(b - \frac{\alpha}{2}\right), \tag{52}$$

where

$$b = \frac{(p_{O_2})_O}{(p_{NO})_O}. \tag{53}$$

Because of stoichiometry, if the reduction in the partial pressure of NO is $(p_{NO})_O \alpha$, then the reduction in partial pressure of O_2 is $(p_{NO})_O \alpha/2$.

Integration of Eq. 51 gives

$$\frac{1}{(1-2b)^2} \ln \frac{2b(1-\alpha)}{(2b-\alpha)} + \frac{1}{(2b-1)} \left(\frac{\alpha}{1-\alpha}\right) = \frac{k_p (p_{NO})_O^2 \tau}{2}, \tag{54}$$

where τ is the residence time for conversion α. Now, this oxidized gas is introduced in the absorption section. It has been pointed out earlier that the absorption of tetravalent NO_x is very fast and the packed volume requirement is very small.

Case 2: Simultaneous Oxidation and Absorption. In addition to the assumptions made in Case 1, we assume that the rate of absorption of product $NO_2 \gg$ the rate of oxidation. This condition is satisfied when the value of effective interfacial area is high (say $> 50\ m^2/m^3$). Because of equilibrium, NO_2 can be in the form of NO_2, N_2O_3, HNO_2, HNO_3, and N_2O_4. The last two forms need not be considered, since we have selected conditions in such a way that nitrite selectivity $> 99\%$. Further, we need to consider that during absorption one mole of NO_2 picks up one mole of NO. With this, Eq. 52 takes the following form:

$$-\frac{dp_{NO}}{dt} = 2\, k_p (p_{NO})_O^3 (1-\alpha)^2 \left(b - \frac{\alpha}{4}\right). \tag{55}$$

It can be noted that k_p in Eq. 55 has been doubled as compared to Eq. 52. This is because the rate of reduction of NO partial pressure doubles in the presence of absorption. Integration of Eq. 55 gives

$$\frac{1}{(1-4b)^2} \ln \frac{(4b)(1-\alpha)}{(4b-\alpha)} + \frac{1}{4b-1} \frac{\alpha}{1-\alpha} = \frac{k_p (p_{NO})_O^2 \tau}{2}. \tag{56}$$

The most important difference between the preceding two cases is that, for a given level of overall conversion α, in Case 1 the extent of oxidation needed is only $\alpha/2$. The product NO_2 (equivalent to $\alpha/2$) picks up an additional amount of NO ($\alpha/2$) in the absorption section. The absorption is considered to be fast, and a small volume is needed for absorption as compared to oxidation. In Case 2, the entire process of NO removal is controlled by oxidation and the extent of conversion is α itself. Table 5 gives the values of τ at different values of α and different levels of NO. From the table it can be seen that the values of τ are much lower for Case 1, mainly because of the conversion level. Second, the average partial pressure of NO during the oxidation stage is higher in Case 1 than that in Case 2. However, we cannot consider all

Table 5. Comparison of Values of τ for Case (i): Oxidation and Absorption in Series and Case (ii): Simultaneous Oxidation and Absorption

	τ (s)					τ (s)			
	Case (i)					Case (ii)			
α	Extent of Oxidation in Case (i)	NO_x 91000 (ppm)	NO_x 30000 (ppm)	NO_x 10000 (ppm)	NO_x 3000 (ppm)	NO_x 91000 (ppm)	NO_x 30000 (ppm)	NO_x 10000 (ppm)	NO_x 3000 (ppm)
0.1	0.05	0.264	2.575	23.83	258	0.512	4.99	46.23	499.92
0.5	0.25	1.805	17.6	162	1761	7.27	70.96	657	7099.95
0.8	0.4	3.868	37.75	349	3776	16.33	159	1474	15942
0.9	0.45	4.876	47.56	440	4759	28.97	283	2615	28280
0.95	0.475	5.476	53.42	494	5345	63.56	620	5736	62038
0.99	0.495	5.993	58.46	541	5850	346	3372	31192	337320
0.995	0.4975	6.099	59.49	551	5953	701	6843	63311	684664

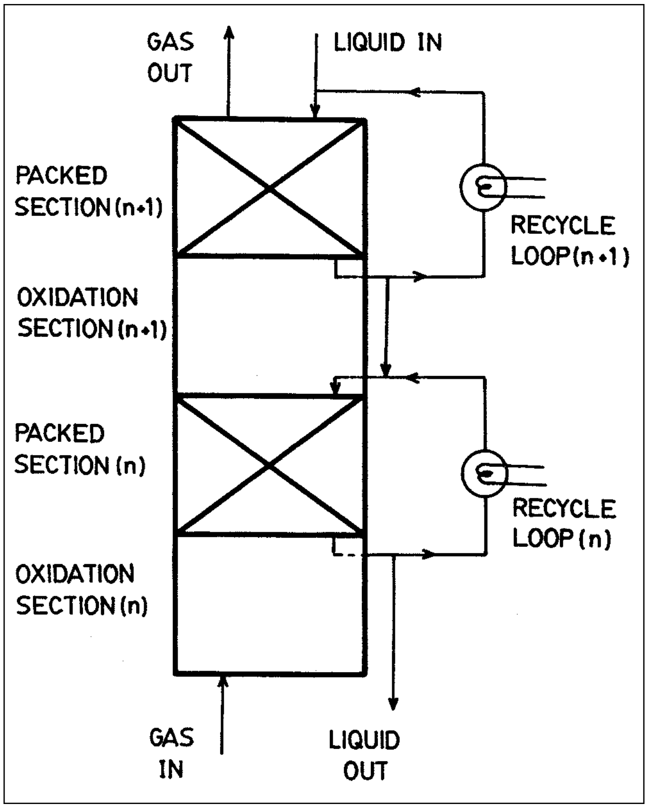

Figure 9. A system with oxidation and absorption carried out simultaneously.

levels of α in Case 1. For the cases with an asterisk, the NO^*/NO_2^* ratio after oxidation is below the critical value and selectivity becomes hampered. This suggests the need for multiple stages of oxidation and absorption. In each stage, oxidation is limited by the desired selectivity. Such a configuration is expected to result in much smaller volumes than in Case 2. Further, in Case 1, the majority of the column volume is empty, so the corresponding cost of the packings is saved. For Case 1, however, we need to size the oxidation and absorption volumes of all the stages in such a way that (1) the extent of oxidation should be as high as possible in order to get the benefit of the higher partial pressure of NO and the rate of oxidation. However, it should not exceed the critical ratio (2); that is, the extent of absorption should be such that the rate of absorption is higher than the rate of oxidation. In other words, for the optimum design, the absorption section should mainly be used for absorption (some oxidation may occur simultaneously) and the oxidation section for oxidation. Further optimization depends upon the levels of oxidation and absorption in the respective sections.

Optimization of the oxidation and absorption sections

In the preceding subsection, it was shown that the total column volume is less when the oxidation and absorption are carried out separately. It was also pointed out that, for the desired level of selectivity, multiple stages of oxidation and absorption may be needed. Figure 9 shows multiple stages of oxidation and absorption. Each stage needs to be optimized for a given level of NO_x, temperature, O_2/NO ratio, and total pressure. For estimating the absorption height, different extents of absorption were considered. For estimating the oxidation height, the extent of oxidation was up to a critical ratio corresponding to the level of NO concentration. The results are given in Table 6. In all the cases, it was ensured that the selectivity was 99%. From Table 6 it can be seen that the absorption heights increase with an increase in the extent of absorption. The oxidation height depends upon the corresponding critical ratio. The optimum combination appears to be when the extent of absorption is in the range of 99.95%. Of course, this optimum level of absorption is for the critical level of oxidation. Further, in the total height, the major portion is that of the oxidation height. Therefore, we thought it desirable to explore the possibility of reducing the oxidation height at every stage. (This will also ensure selectivity, because the NO^*/NO_2^* will always be above the critical values.) The results are shown in Table 7. It can be seen that the total height can be reduced considerably by proper selection of the oxidation and absorption heights.

The effect of absorption height is shown in Tables 6 and 7. Alternatively, we considered investigating the sensitivity of the oxidation height. Figure 10 shows the results for the case of 1-m packed height. The effect of three inlet concentrations is also shown. In all cases, an optimum oxidation height can be observed. The optimum becomes higher when the inlet ratio NO^*/NO_2^* is increased.

Table 6. Height of Oxidation and Packed Section for Different Levels of Absorption and Oxidation up to Critical Ratio

% Absorption	Absorption Heights	Oxidation Heights	Total Height
95	$0.35+5.75+3.25+2.70+2.55+2.50+2.50=19.60$	$2.65+5.29+9.43+14.85+22.95+35.02=90.19$	109.79
98	$0.35+9.1+4.5+3.25+2.99+2.89=23.08$	$4.04+8.63+14.41+22.92+35.6=85.60$	108.68
99	$0.35+12.35+6.75+3.55+3.25=26.25$	$5.36+11.7+19.31+30.6=66.97$	93.22
99.90	$0.35+30.15+28.7=59.20$	$13.36+32.55=45.91$	105.11
99.92	$0.35+32.65+33=66$	$14.41+35.93=50.34$	116.34
99.93	$0.35+34.3=34.65$	15.1	49.75
99.95	$0.35+38.65=39$	16.9	55.90
99.99	$0.35+67.89=68.24$	29.14	97.38

Note: Inlet NO_x concentration = 91,000; outlet NO_x concentration = 2000 ppm; temperature = 50°C; total pressure = 0.1 MPa; $b=0.82$.

Table 7. Total Height Requirement with Respect to Different Extents of Absorption and Oxidation

Extent of Absorption (%)	Extent of Oxidation in Terms of NO^*/NO_2^* at the End of Oxidation			
	4	5.67	6.5	7
98	111.18	109.14	92.93	86.76
99	78.6	91.47	83.70	80.53
99.50	99	78.75	103.51	108.77
99.90	103.51	104.77	105.72	106.30
99.92	114.72	116	117.05	44.47
99.93	121.99	49.40	47.58	46.69
99.95	62.18	55.98	53.53	52.54
99.99	108.26	97.03	93.57	90.90

Note: Inlet NO_x concentration = 91,000 ppm; outlet NO_x concentration = 2000 ppm; temperature = 50°C; pressure = 0.1 MPa; $b = 0.82$; other details are given in the numbered list in the third section.

Conclusions

1. A mathematical model was developed for the absorption of NO_x gases in aqueous NaOH solutions. Procedures were given for estimating the overall reaction rates and the selectivity.

2. The parametric sensitivity of temperature, pressure and NO_x composition on the rates and selectivity was examined in detail. It was shown that the two objectives of rate and selectivity make opposite demands on the operating parameters, such as temperature, pressure, and NO_x composition. The most important parameter governing the selectivity and the rate is the NO^*/NO_2^* ratio, which in turn may depend upon temperature, total pressure, and NO_x partial pressure.

3. In the range of conditions covered in this work, the major absorption occurs via HNO_2 (Eq. 22) followed by N_2O_3 (Eqs. 20 and 35). The reduction in selectivity (that is, nitrate formation) was found to depend mainly on water pressure in the gas phase. The higher partial pressure favors the formation of HNO_3, and hence sodium nitrate. These two rates explain the importance of various parameters, such as the NO^*/NO_2^* ratio, the partial pressure of NO_x, temperature, and pressure.

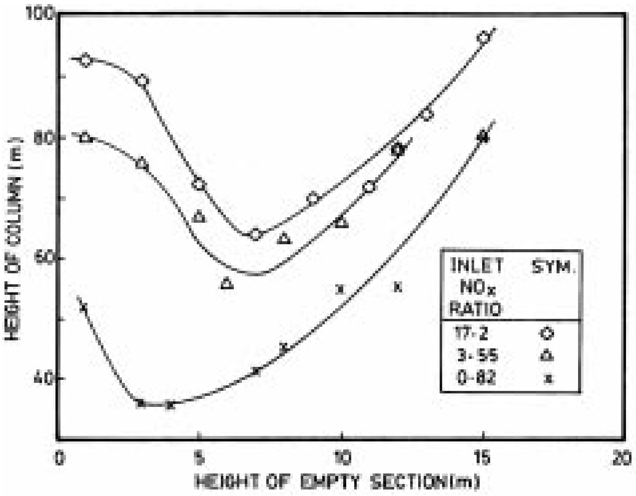

Figure 10. Effect of oxidation height on total height of column for given packed height.

Packed height = 1 mm; inlet concentration of total NO_x = 91,000 ppm; outlet concentration of NO_x = 2000 ppm; pressure = 0.1 MPa; $b = 0.82$.

4. The strategy of simultaneous oxidation and absorption was shown to be inferior to the strategy of separate stages of oxidation and absorption.

5. An optimum design strategy was presented by considering the different extents of absorption and oxidation and by properly configuring the oxidation and absorption sections.

6. A very good agreement was found between the model predictions and the performance of the two operating plants.

Acknowledgments

One of the authors (M.P.P.) thanks the University Grant Commission for the award of a fellowship.

Notation

a_p = dry surface area, m^2/m^3
b = molar ratio of oxygen to nitric oxide
dp = diameter of packing, mm
D_G = gas-phase diffusivity, m^2/s
D_x = diffusivity of component x, m^2/s
f = friction factor
k_p = rate constant for NO oxidation
L_T = scale of turbulence, m
L_Y = molar flow rate of liquid, kmol/s
P_I = partial pressure of inerts, kN/m^2
P_M = power consumption per unit mass, W/kg
P_T = total pressure of gas, kN/m^2
R = universal gas constant, $m^3\ (kN/m^2)/(kmol/K)$
S = cross-section area of column, m^2
Sc_G = Schmidt number
V_G = superficial gas velocity, m/s
V_L = superficial liquid velocity, m/s
$(X_{OH^-})_Y$ = moles of hydroxide per moles of inerts
$(X_{NO_2^-})_Y$ = moles of nitrite per moles of inerts

Greek letters

α = fractional conversion of nitric oxide
ϵ_G = fractional gas holdup
ϵ_L = fractional liquid holdup
μ_G = viscosity of gas
ρ_G = density of gas, kg/m^3

Subscripts

L = liquid phase
x = NO, NO_2, N_2O_3, N_2O_4, HNO_3, HNO_2, H_2O, O_2
y = streams A, B, C, D, E

Literature Cited

Bodenstein, M., "Formation and Dissociation of Higher Nitrogen Oxide," *Z. Phys. Chem.*, **100**, 68 (1922).

Carta, G., "Role of HNO_2 in the Absorption of Nitrogen Oxides in Alkaline Solutions," *Ind. Eng. Chem. Fundam.*, **23**, 260 (1984).

Counce, R. M., and J. J. Perona, "Scrubbing of Gaseous Nitrogen Oxides in Packed Towers," *AIChE J.*, **29**, 26 (1983).

Jethani, K. R., N. J. Suchak, and J. B. Joshi, "Modeling and Simulation of a Spray Column for NO_x Absorption," *Comput. Chem. Eng.*, **16**, 1 (1992).

Joshi, J. B., V. V. Mahajani, and V. A. Juvekar, "Absorption of NO_x Gases," *Chem. Eng. Commun.*, **33**, 1 (1985).

Kameoka, V., and R. L. Pigford, ''Absorption of Nitrogen Oxide into Water, Sulphuric Acid, Sodium Hydroxide and Alkaline Sodium Sulphite Aqueous Solutions,'' *Ind. Eng. Chem. Fundam.*, **16**, 163 (1977).

Komiyama, H., H. Inoue, H. Tanaka, and M. Aoki, ''Simultaneous Absorption of NO and NO_2 into Alkaline Solutions,'' *J. Chem. Eng., Jpn.*, **15**, 362 (1982).

Perry, R. H., and C. H. Chilton, *Chemical Engineer's Handbook*, McGraw-Hill, Kogakusha, Tokyo, p. 3 (1984).

Pradhan, M. P., N. J. Suchak, P. R. Walse, and J. B. Joshi, ''Multicomponent Gas Absorption with Multiple Reactions: Modeling and Simulation of NO_x Absorption in Nitric Acid Manufacture,'' *Chem. Eng. Sci.*, **52**, 4569 (1997).

Schwartz, S. E., and W. H. White, ''Solubility Equilibria of the Nitrogen Oxides and Oxyacids in Dilute Aqueous Solutions,'' *Adv. Environ. Sci. Eng.*, **4** (1981).

Suchak, N. J., K. R. Jethani, and J. B. Joshi, ''Absorption of Nitrogen Oxides in Alkaline Solutions: Selective Manufacture of Sodium Nitrite,'' *Ind. Eng. Chem. Res.*, **29**, 1492 (1990).

Suchak, N. J., K. R. Jethani, and J. B. Joshi, ''Modeling and Simulation of NO_x Absorption in Pilot-Scale Packed Columns,'' *AIChE J.*, **37**, 3 (1991).

Manuscript received Jan. 13, 1998, and revision received Nov. 5, 1998.